

A Study on a Thixoforming Process Using the Thixotropic Behavior of an Aluminum Alloy with an Equiaxed Microstructure

C.G. Kang and H.K. Jung

(Submitted 13 March 2000)

Alloys with an equiaxed microstructure exhibit significantly lower flow resistance in the semisolid state than alloys with a dendritic microstructure. Their thixotropic behavior (solidlike in the unperturbed state and liquidlike during shearing) has been the basis for a thixoforming process. It is accepted today that thixoforming is a new net-shaped manufacturing technology in which the billet is heated to the semisolid state with coexisting solid-liquid phases.

The thixoforming process has some industrial advantages, such as the successful fabrication of high-quality components with fewer inner defects, suitable for less machining, high productivity comparable to high-pressure die casting, and being an energy-saving system without the conventional melting process. It consists of inductive coil design, a billet reheating process, billet handling, filling into the die cavity, and solidification of the thixoformed part.

This work presents an overview of all the detailed stages in the thixoforming process to manufacture the net-shaped product with good mechanical properties. An air compressor part with high strength has been fabricated by the thixoforming process.

Keywords equiaxed microstructure, globular microstructure, thixotropic behavior, thixoforming process

1. Introduction

To achieve the production of lightweight parts, several technologies, such as the development of tailored alloys[1,2] coinciding with the requirements of the components, process design[3,4] for the manufacturing process, and die design,[5] must be mutually connected.

From this point of view, the outstanding necessity for vehicle weight reduction has led to a major increase in aluminum alloy production of mechanical components for automobile applications. In addition, a large number of studies related to thixoforming, which is one of the methods manufacturing net-shaped products, has been actively conducted.[6–12]

In a study of the thixoforming process, Young and Fitze[7] compared qualitatively defects of the products manufactured by high-pressure casting and semisolid die casting and reported examples in the development of several automobile parts. Midson *et al.*[13] proposed that a coil design used for induction heating of the semisolid was necessary for uniform induction heating. Jung *et al.*[3,14] developed an automatic quadrilateral mesh generator with automatic mesh refinement to meet special demands found in the thixoforming process analysis with arbitrarily shaped dies by the renumbering and modifications of the nodal position. Jung and Kang[1,2,4,6] proposed the JKK objective function for the variation of weight values by introducing an optimization technique and experimentally verifying the suitability of an optimization of the inductive coil design by applying the induction heating experiment to obtain a fine globular microstructure suitable for thixoforming.

It is especially important to prevent defects such as liquid segregation, shrinkage pores, and nonfilling. Studies on the construction of a reheating database and die design for the thixoforming process have not been reported yet, and practical use of a conventional commercial package is extremely restricted.

So, in this work, the results of inductive coil design and numerical simulation were used to fabricate aluminum frame products with the required strength and wear resistance by the thixoforming process. Two models were suggested for the variation of the gate shape considered in die design by the numerical simulation, and a filling pattern for them was calculated and applied to the die design. Experiments to determine the effects of variation of die temperature, pressure, and pressing holding time were performed. The sample frame products were evaluated by investigating the mechanical properties of the fabricated aluminum frame products such as hardness and wear resistance.

Table 1 Designed dimensions of the induction heating device ($f = 60$ Hz, and $\delta = 10.7$ mm)

Alloy	Billet diameter (d: mm)	Coil inner diameter (D_i: mm)	Minimum heating length (l_w: mm)	Optimal coil length (H: mm)	Coil wall thickness: (d_c: mm)
A356	76	100	93	118–168	10

H.K. Jung and **C.G. Kang**, School of Mechanical Engineering, Engineering Research Center for Net Shape and Die Manufacturing, Pusan National University, Pusan, 609-735, Korea. Contact e-mail: cgkang@hyowon.pusan.ac.kr (C.G. Kang), hongkyu@lycos.co.kr (H.K. Jung).

2. Inductive Coil Design

2.1 The Aims of Inductive Coil Design

During induction heating, the relationship between time and temperature must be controlled exactly to obtain a uniform temperature distribution over the entire cross-sectional area. Because the initial eutectic temperature (*i.e.*, initial solid fraction) in the thixoforming process is the key parameter to filling results in the thixoforming process, an accurately controllable induction heating method must be selected for the reheating process.

For the thixoforming process, the reheating of the billet into the semisolid state as quickly and homogeneously as possible is one of the most decisive aspects. From this point of view, the design of the induction coil is very important. For a real system consisting of a coil and billet, the heat induced over the length of the billet is normally not equally distributed, and, consequently, there is a nonuniform temperature distribution. So an important point for optimization of coil design is to verify the correct relationship between coil length and billet length.[1,2,4,6]

2.2 Optimal Coil Design

The optimal coil length H and coil inner diameter Di of an induction heating system were designed for uniform reheating. The coil dimensions for aluminum alloy A356 with $d \times l = 76 \times 90$ mm are described in Table 1, where δ is the depth of penetration of the current (the skin depth).

The suitability of an optimal coil design was verified through the finite element modeling (FEM) simulation of the induction heating process by using a general purpose finite element analysis code, ANSYS™.[4,6,15] The results of the simulation show that using coils that are too long leads to overheating of the corners of the billet, whereas coils that are too short mainly heat the billet's middle part. From the above results, we found the coil dimension to minimize the electromagnetic end effect is a length of 120 mm, 30 mm longer than the billet length.

3. Reheating Experiments

3.1 The Experimental Method

The starting material used in this study was an aluminum alloy, A356, fabricated by the electromagnetic stirring process and made by Pechiney (Voreppe, France). The chemical composition is shown in Table 2, and the microstructure of the raw material with equiaxed grains is shown in Fig. 1. The induction heating system consists of a variable-frequency induction furnace that allows more uniform temperatures to be established

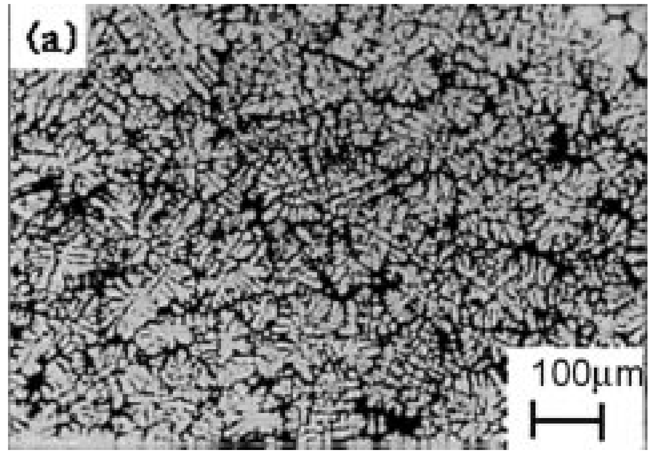

Fig. 1 Optical micrograph of starting material, aluminum alloy A356

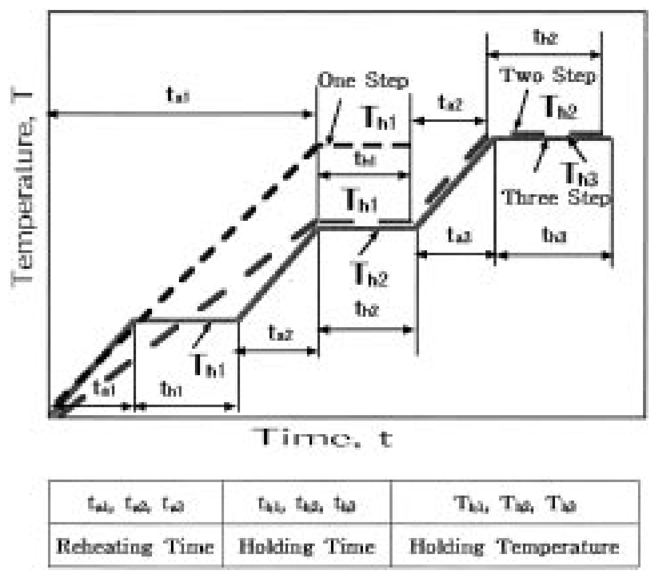

Fig. 2 Input data diagram of reheating conditions to obtain the globular microstructure suitable for thixoforming

Table 2 Chemical composition of A356

	Si	Fe	Cu	Mn	Mg	Cr	Zn	Ti	Pb	Al
Min (%)	6.5	…	…	…	0.30	…	…	…	…	
Max (%)	7.5	0.15	0.03	0.03	0.40	…	0.05	0.20	0.03	bal

Table 3 The reheating conditions for semisolid aluminum alloy (A356 with $d \times l = 76 \times 90$ mm)

	Reheating time t_a(min)			Holding temperature T_k (°C)			Holding time t_k (min)				
Alloy	t_{a1}	t_{a2}	t_{a3}	T_{k1}	T_{k2}	T_{k3}	t_{k1}	t_{k2}	t_{k3}	Total time (min)	Capacity Q (kW)
A356	4	3	1	350	570	576	1	3	2	14	12.04

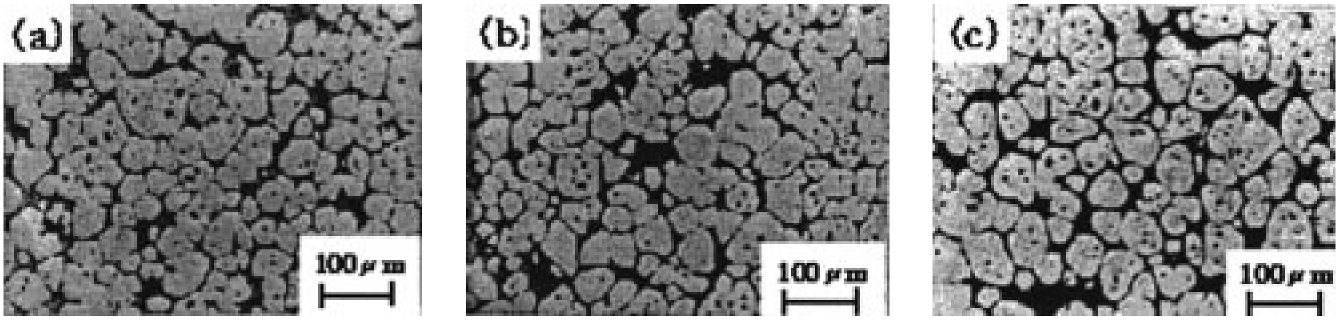

Fig. 3 Microstructure obtained in a three-step reheating process for thixoforming with A356 alloy (f_s = 55%, t_{a1} = 4 min, t_{a2} = 3 min, t_{a3} = 1 min, T_{h1} = 350 °C, T_{h2} = 570 °C, T_{h3} = 576 °C, t_{h1} = 1 min, t_{h2} = 3 min, t_{h3} = 2 min, and Q = 12.04 kW)

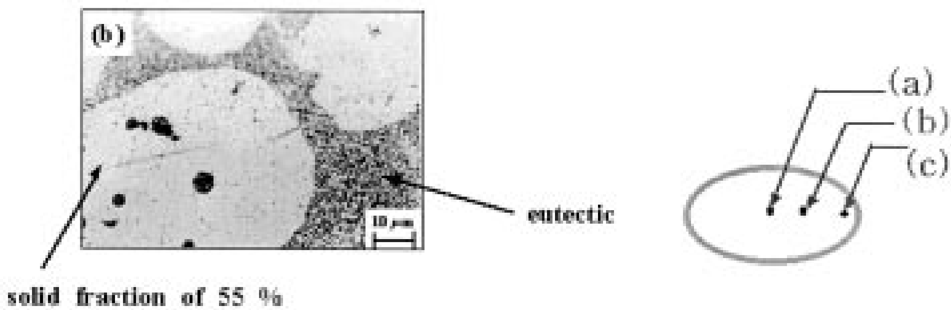

Fig. 4 Eutectic microstructure of A356 alloy (ALTHIX) after reheating to the semisolid state (f_s = 55%, t_{a1} = 4 min, t_{a2} = 3 min, t_{a3} = 1 min, T_{h1} = 350 °C, T_{h2} = 570 °C, T_{h3} = 576 °C, t_{h1} = 1 min, t_{h2} = 3 min, t_{h3} = 2 min, and Q = 12.04 kW) and positions for microstructure observation

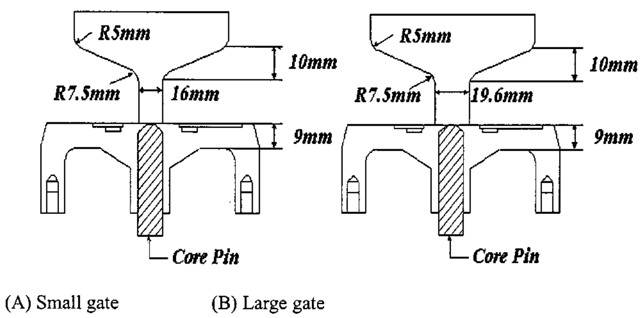

Fig. 5 Gate dimensions for the variation of gate shape

during partial melting of billets. The frequency can be varied from 60 to 3 kHz, with a maximum power of 50 kW, providing flexibility in the range of aluminum alloys that can be partially melted after machining the A356 alloy to $d \times l = 76 \times 90$ mm.

To achieve uniform heating, the optimal heating coil of the induction heating system based on the FEM simulations was made by winding a copper tube to $D_0 \times H = 120 \times 120$ mm.[15,16] Thermocouple holes to measure the temperature accurately were machined to 2 mm diameter at a position 45 mm from the surface of the billet and 2 mm diameter at a position 10 mm from the lateral of the billet. To accurately control the temperature of the billet, type K thermocouples of ϕ 1.6 mm were inserted into the billet. The heating temperature was set to the datum as a thermocouple position (b) in Fig. 4. Table 3 shows the optimal reheating conditions of A356 with $d \times l = 76 \times 90$ mm. The meanings of the symbols used in Table 3 are the same as those shown in Fig. 2.

3.2 The Results of the Reheating Experiment and Discussion

Figure 3 shows a fine globular microstructure of the A356 alloy. Heat was achieved under the reheating conditions. Figure 4 shows the micrograph magnified to the scale of 1000 to observe the eutectic microstructure of Fig. 3, which obtained the finest globular microstructure for a solid fraction, an *fs* of 55%. Figure 4 shows that the eutectic is melted completely. Therefore, it was found that a temperature of 575 °C was needed for complete melting of the eutectic. Before and after the melting of the eutectic, the solid fraction changes rapidly and a rapid temperature rise occurs when the liquid phase forms. Because of this temperature rise, controlling the reheating temperature is difficult. Therefore, to homogeneously control the temperature distribution and the solid fraction of the work piece, the billet must be reheated in three steps.

4. Die Design

4.1 Filling Simulation

The filling analysis by numerical simulation was performed. After modeling an aluminum frame by numerical simulation, the temperature and pressure fields were calculated by the commercial package, MAGMA S/W V.3.5 (Thixo Module, MAGMA GmbH, Aachen, Germany), which can be applied in the case of thixoforming.

The analyses were carried out for two gate shapes with models I (small gate) and II (large gate), as shown in Fig. 5.

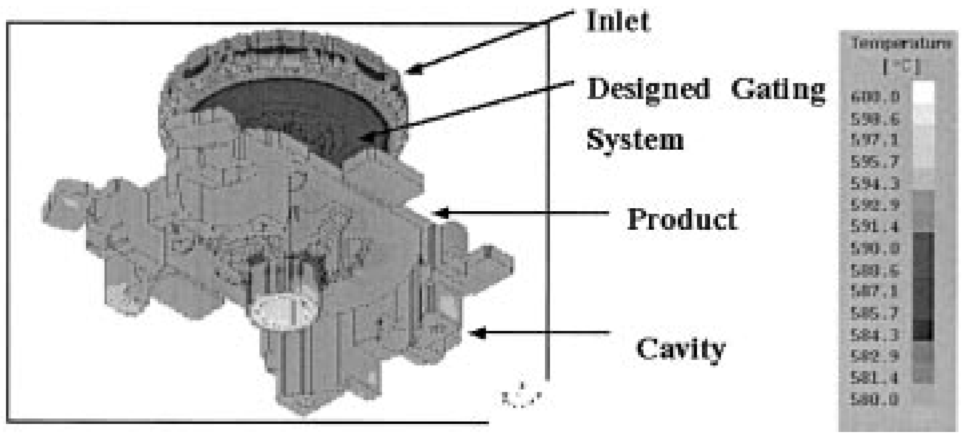

(**a**) Temperature distribution

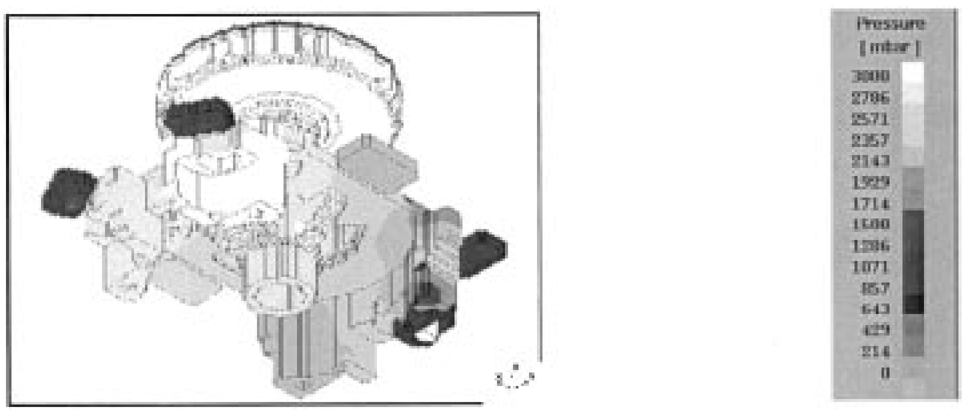

(**b**) Pressure distribution

Fig. 6 Temperature and pressure distributions for small gate (100% filled): (**a**) temperature distribution and (**b**) pressure distribution

Ram speed was fixed as $V_{\text{die}} = 300$ mm/s and initial billet and die temperatures were set at 577 and 300 °C, respectively. The filling analysis was performed at the heat transfer coefficients of 500 W/m^2 K for the surfaces between mold and mold and 1000 W/m^2 K for the surfaces between cast and mold.

4.2 The Results of the Filling Simulation

Figure 6 and 7 show the temperature and pressure distributions of small and large gates when filling is completed. From the results of the filling simulations, it is found that they show the characteristic features of thixotropic flow behavior and coincide with the real patterns of flow and filling into the die cavity. As shown in Fig. 6 and 7, model I (small gate), where the flow and pressure are distributed more uniformly entirely, is better for a die design in terms of preventing liquid segregation. Those facts would be very useful for thixoforming practitioners and engineers in determining the geometry (shape and dimensions) of the gating system and die cavity.

5. Thixoforming Experiments

The servohydraulic thixoforming press at the Engineering Research Center for Net Shape and Die Manufacturing, Pusan National University (ERC/NSDM), has the capacity for producing a 737 MPa load (main cylinder: 421 Mpa, and bottom cylinder: 316 MPa) during forming. The press is computer controlled and equipped with a digital control system that provides real-time data acquisition, saved to the computer's hard disk drives. The user can choose a number of process variables such as the velocity profile of the ram during the billet injection into the die cavity or the magnitude of the applied load and the time duration of its application (pressing holding time).

Figure 8 shows the picture of the specimen for a tensile test. Figure 9 shows the ultimate strength for a variety of forming conditions and heat treatment conditions. The forming conditions and heat treatment conditions are described in Tables 4 and 5. Experiments 6, 13, and 15 were performed under the conditions of billet temperature (T_m) at 580 °C and die temperature (T_d) at 250, 300, and 350 °C, respectively, and experiment 7 was formed at 582 and 250 °C. In the case of a non-heat-treated product, a maximum ultimate tensile strength of 285 MPa was measured at the conditions of experiment 12 (T_m: 577 °C, and T_d: 300 °C). On a tensile test, it was also observed that the ultimate strengths of the T5 heat-treated aluminum frame product (324 MPa) and the T6 heat-treated product (394 MPa) were approximately 13% and 38% superior to that of the non-heat-treated product, respectively.

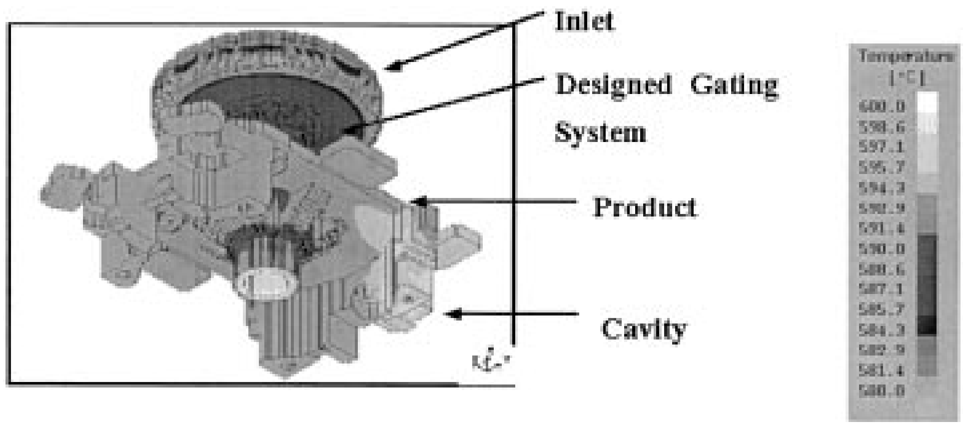

(**a**) Temperature distribution

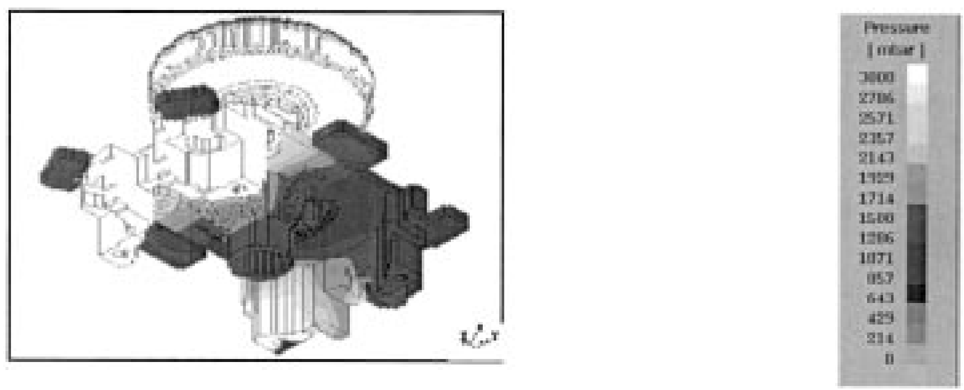

(**b**) Pressure distribution

Fig. 7 Temperature and pressure distributions for large gate (100% filled): (**a**) temperature distribution and (**b**) pressure distribution

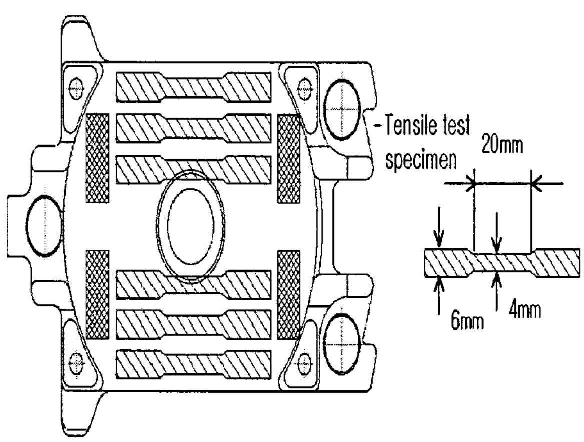

Fig. 8 Specimen dimensions for a tensile test

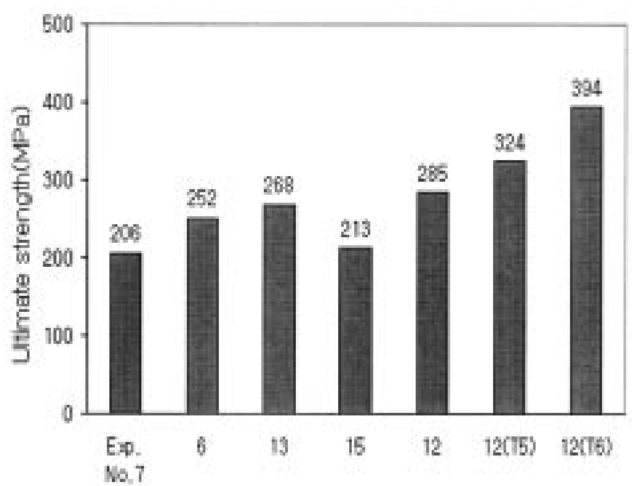

Fig. 9 Ultimate tensile strength distribution for the variation of forming conditions and heat treatment conditions. (The forming conditions and heat treatment conditions are described in Tables 4 and 5)

Defects of products occurring during thixoforming are unfilling phenomena in the die filling, oxide films, segregation of eutectic α, coarsening of primary α, shrinkage pore, *etc.*[1,2,5,17–20] In this work, where we used the inductive coil design based on the finite element analysis and the die design based on the numerical simulation, in the case where filling was finished, the above-mentioned defects were not observed. We suggest that thixoforming technologies including an optimal coil design and the die design for avoiding liquid segregation proposed in this work would contribute to the reduction of many lead times for manufacturing.

Table 4 Thixoforming conditions (pressing pressure: 80 MPa, and pressing holding time: 20 s)

Experiment Number	Die temperature T_d (°C)	Billet temperature T_m (°C)	Injection velocity V (mm/s)
1	200	577	160
2	200	582	160
3	200	577	300
4	250	577	160
5	*250*	*577*	*300*
6	250	580	300
7	250	582	300
8	280	577	160
9	280	580	160
10	300	577	160
11	300	580	160
12	*300*	*577*	*300*
13	300	580	300
14	350	580	160
15	350	580	300

Table 5 Heat treatment conditions for thixoformed product

Type	Solutionizing	Cooling	Aging	Cooling
T5	None	Water quenching on stripping	6 h-170 °C	Air cooling
T6	10 h-540 °C	Water quenching	6 h-170 °C	Air cooling

6. Conclusions

This paper has presented all of the thixoforming processes from the optimal coil design for uniform heating to the gate design to obtain good mechanical properties during thixoforming. The conclusions can be summarized as follows:

- The optimal coil dimensions for a commercial induction heating system to produce uniform heating were proposed for 60 Hz, often used in the thixoforming process.
- The optimal reheating conditions for A356 alloy were proposed to obtain a fine globular microstructure suitable for thixoforming.
- From the results of filling simulations, it was found that they showed the characteristic features of thixotropic flow behavior. The filling patterns into the die cavity coincided with the real flow.
- In the case of a non-heat-treated product, a maximum ultimate tensile strength of 285 MPa was measured at the conditions of experiment 12 (T_m: 577 °C, and T_d: 300 °C). On a tensile test, it was also observed that the ultimate strengths of the T5 heat-treated aluminum frame product (324 MPa) and the T6 heat-treated product (394 MPa) were approximately 13 and 38% superior to that of non-heat-treated product, respectively.

Acknowledgments

The authors express heartfelt thanks for financial support to the ERC/NSDM, which is an excellent center appointed by the Korean Science and Engineering Foundation. All work was done at the Materials Processing Control Laboratory (MPC Lab) of Pusan National University.

References

1. H.K. Jung and C.G. Kang: *Metall. Mater. Trans. A*, 1999, vol. 30A, pp. 2967-77.
2. H.K. Jung and C.G. Kang: *J. Kor. Foundrymen's Soc.*, 1999, vol. 19 (3), pp. 225-35.
3. C.G. Kang and H.K. Jung: *Int. J. Mech. Sci.*, 1999, vol. 41 (12), pp. 1423-45.
4. H.K. Jung and C.G. Kang: *Key Eng. Mater.*, 2000, vol. 177-180, pp. 571-76.
5. C.G. Kang, H.K. Jung, and K.W. Jung: *Proc. Int. Symp. on Advanced Forming and Die Manufacturing Technology (AFDM'99)*, C.G. Kang and Y.H. Moon, eds., Pusan National University, Pusan, Korea, 1999, pp. 83-88.
6. C.G. Kang, H.K. Jung, and Y.J. Jung: *Adv. Technol. Plasticity*, 1999, vol. 3, pp. 1689-94.
7. K.P. Young and R. Fitze: *Proc. 3rd Int. Conf. on Semi-Solid Processing of Alloys and Composites*, M. Kiuchi, ed., Tokyo University, Tokyo, Japan, 1994, pp. 155-77.
8. P. Kapranos, R.C. Gibson, D.H. Kirkwood, and C.M. Sellars: *Proc. 4th Int. Conf. on Semi-Solid Processing of Alloys and Composites*, D.H. Kirkwood and P. Kapranos, eds., The University of Sheffield, Sheffield, UK, 1996, pp. 148-52.
9. W. Kahrmann, R. Schragner, and K. Young: *Proc. 4th Int. Conf. on Semi-Solid Processing of Alloys and Composites*, D.H. Kirkwood and P. Kapranos, eds., The University of Sheffield, Sheffield, UK, 1996, pp. 154-58.
10. D.H. Kirkwood: *Int. Mater. Rev.*, 1994, vol. 39 (5), pp. 173-89.
11. G. Clauser, A. Ravaioli, F. Ciselli, and M. Vassallo: *Proc. 4th Int. Conf. on Semi-Solid Processing of Alloys and Composites*, D.H. Kirkwood and P. Kapranos, eds., The University of Sheffield, Sheffield, UK, 1996, pp. 234-38.
12. T. Witulski, A. Winkelmann, and G. Hirt: *Proc. 4th Int. Conf. on Semi-Solid Processing of Alloys and Composites*, D.H. Kirkwood and P. Kapranos, eds., The University of Sheffield, Sheffield, UK, 1996, pp. 242-46.
13. S. Midson, V. Rudnev, and R. Gallik: *Proc. 5th Int. Conf. on Semi-Solid Processing of Alloys and Composites*, A.K. Bhasin, J.J. Moore, K.P. Young, and S. Midson, eds., Colorado School of Mines, CO, 1998, pp. 497-504.
14. C.G. Kang, N.S. Kim, and H.K. Jung: *Proc. 6th Int. Conf. on Semi-Solid Processing of Alloys and Composites*, M. Rosso and G. Chiarmetta, eds., Turin (Italy), Sept. 27-29th, Unione Industriale di Torino, Turin, Italy, 2000, in press.
15. H.K. Jung, N.S. Kim, and C.G. Kang: *J. Kor. Foundrymen's Soc.*, 1999, vol. 19 (5), pp. 393-402.
16. H.K. Jung, C.G. Kang, and Y.H. Moon: *J. Mater. Eng. Performance*, 2000, vol. 9 (1), pp. 12-23.
17. G. Hirt, R. Cremer, A. Winkelmann, T. Witulski, and M. Zillgen: *J. Mater. Processing Technol.*, 1994, vol. 45, pp. 359-64.
18. W.R. Loué and M. Garat: *Proc. Symp. on Forming Technology of Semi-Solid Metals*, C.G. Kang, ed., Pusan National University, Pusan, Korea, 1997, pp. 96-104.
19. C.G. Kang, S.S. Kang, and H.K. Jung: *Adv. Technol. Plasticity*, 1999, vol. 3, pp. 1701-06.
20. H.K. Jung and C.G. Kang: *Key Eng. Mater.*, 2000, vol. 177–180, pp. 565-70.